Green synthesis of Fe-Ni bimetallic material from guava leaf extract for Cu removal from wastewater

Dinh Thi Lan Phuong[1*], Tran Thi Thu Ha

Abstract: This study synthesized Fe-Ni bimetallic material from the guava leaf extract for the removal of copper (Cu) from wastewater. The material composition was characterized using EDS and FT-IR spectra. SEM images indicated that particle sizes ranging from 60 to 90 nm, confirming the nanoscale nature of the material. Batch adsorption experiments were conducted with an initial Cu concentration in solution of 5 mg/L. The results showed that Fe-Ni exhibited Cu removal capability, as evidenced by EDS and FT-IR analyses after the adsorption process. The removal mechanism was proposed to involve adsorption and reduction processes on the material surface. Optimal conditions were found to be pH 6, Fe-Ni dosage of 0.8 g/L, temperature of 25°C, contact time of 150 minutes, achieving a maximum removal efficiency of 79%. These results suggest that Fe-Ni synthesized from guava leaves is a friendly and low-cost adsorbent with strong potential for Cu removal in water treatment applications.

Keywords: Fe-Ni bimetallic material, Cu removal, wastewater treatment, adsorption, green synthesis.

1. Introduction

Copper (Cu) pollution resulting from inadequately regulated effluents discharged by electroplating and metallurgical industries has become increasingly severe in recent years (Hamdi, M.F., 2025). As a non-biodegradable metal, Cu accumulates in the environment and poses significant risks to community health. The current status of Cu pollution in wastewater and sludge in Vietnam has shown an increasing trend in recent years. Alarming levels of contamination have been detected in industrial and urban areas. A study by Van Thinh, N. et al. (2022) in northern Vietnam revealed that sludge from several industrial zones contained Cu concentrations 2 to 10 times higher than those of natural soils. In some industrial facilities equipped with treatment systems, the influent wastewater exhibited an average Cu concentration of approximately 0.11 mg/L, which was reduced to 0.008-0.01 mg/L after treatment (USEPA, 2021). However, many industrial complexes and residential areas still lack wastewater treatment systems. In the coastal areas of the Red River Delta, Cu concentrations in seawater ranged from 0.1 to 96.0 µg/L with an average of 26.91 µg/L, indicating that coastal waters have been affected by uncontrolled discharges from aquaculture activities and terrestrial sources (Le, N.D. et al., 2022). In traditional craft villages such as Van Mon Village (Bac Ninh Province), approximately 30-40 tons of solid waste are generated daily, including aluminum sludge and coal residues from metal smelting processes (MONRE, 2020). Monitoring results of the surface water quality in this area revealed Cu concentrations exceeding the permissible standard by 2.1-3.1 times. Therefore, research on effective methods for Cu removal from aquatic systems is urgently required (Youssif, M.M. et al., 2024).

Among all methods for Cu removal, adsorption is considered a more effective and economical solution due to its simple operation (Sewoon K. et al., 2018; Hamdi, M.F., 2025). The essential requirements for an adsorbent include a large surface area, low diffusion resistance, and short adsorption equilibrium time to efficiently remove substantial amounts of pollutants, while generating minimal sludge to reduce treatment cost (Hamdi, M.F., 2025). Consequently, nanomaterials, with their advantages such as high surface area and enhanced reactivity, have been applied for Cu remediation. Various nanostructured materials, including iron, manganese, aluminum, titanium, and magnesium (Xu, Q. et al., 2017), as well as polyanilinemodified chitosan coated with ZnO/Fe_3O_4, have been successfully utilized for Cu removal due to their large surface area (Rakatiet, K.K. et al., 2019).

However, some synthesis methods for preparing adsorbent materials are often costly. Moreover, certain synthesis approaches require the use of hazardous chemical reagents, which may lead to secondary pollution. Therefore, low-cost and environmentally friendly synthesis methods for pollutant removal have attracted increasing attention. Recently, the use of plant extracts for material synthesis has helped overcome several of these limitations. A key advantage of plant-based synthesis is the utilization of biomolecules present in plant extracts, such as aldehydes, amines, and polyphenols, which act as reducing agents to reduce the oxidation process on the material surface, thereby replacing toxic and potentially explosive chemicals such as $NaBH_4$. Representative studies include Weng et al. (2017), successfully synthesized

[1] Thuyloi university
[2] 63 KTH, Thuyloi university
[*] Corresponding author
Received 20th Aug. 2025
Accepted 28th Oct. 2025
Publication date 31st Dec. 2025

the Fe-Ni bimetallic nanoparticles from eucalyptus leaf extract. In addition, Gao et al. (2019) utilized Ginkgo biloba leaf extract as a stabilizing agent in the synthesis of Fe/Co bimetallic nanoparticles. Similarly, Yuanqiong Lin et al. (2019) synthesized Fe-Ni bimetallic nanoparticles using eucalyptus leaves, achieving a Cu removal efficiency of 44.1% under optimal experimental conditions. Abbas, A. K. K. R. et al. (2024) synthesized Fe-Ni nanoparticles from green tea leaves combined with limestone to remove tetracycline from groundwater. Furthermore, *Xu et al. (2017)* developed nanocomposite materials derived from black locust for the adsorption of Cr(VI), Cu, and Pb(II) from aqueous solutions. Compared with monometallic Fe-based materials, Fe-based bimetallic materials such as Fe/Co and Fe-Ni have been more widely applied in wastewater Cu remediation, as Co and Ni function as catalysts that enhance Cu removal rates by increasing adsorption sites and improving the reductive activity of Fe in the conversion of Cu^{2+} to Cu (Weng et al., 2017). Research on the synthesis of bimetallic materials from plant extracts for Cu removal from wastewater remains limited in Vietnam. Moreover, guava (Psidium guajava L.) is a widely cultivated fruit tree, and its leaves are commonly discarded after harvest, making them an accessible biomass resource. Therefore, this study focuses on the synthesis of Fe-Ni bimetallic materials using guava leaf extract for the removal of Cu from wastewater.

2. Materials and methods

Material: Guava leaves were collected from Thuan An commune, Hanoi. The chemicals used included $FeSO_4.7H_2O$, HNO_3 (68%), $NiCl_2.6H_2O$, anhydrous NaOH, and $CuSO_4$ (> 99%) purchased from Merck.

Material synthesis: The synthesis procedure was adapted from previously reported methods, including the preparation of Fe-Ni bimetallic nanoparticles from eucalyptus leaves (Weng et al., 2017), eucalyptus leaf extract (Yuanqiong Lin et al., 2019), Fe nanoparticles from *Syzygium nervosum* leaves (Phuong D.T.L., 2024), and Fe/Co bimetallic nanoparticles (Gao, J.F. et al., 2019), with further modifications through experimental optimization. Freshly harvested guava leaves were washed thoroughly, air dried, and oven dried at 60°C for 24 h. A total of 50 g of dried leaves was cut into 2-3 cm pieces and transferred into a 1000 mL beaker containing 500 mL of distilled water. The mixture was heated in a water bath at 80°C for 60 min, then cooled and filtered through glass fiber filter paper with a pore size of 0.45 µm to obtain the guava leaf extract.

A mixed solution of $FeSO_4$ (0.1 M) and $NiCl_2$ (0.1 M) was added to the guava leaf extract in a volume ratio of 1:1:4. The mixture was then subjected to ultrasonic agitation at room temperature for 30 minutes, followed by magnetic stirring for an additional 30 minutes until the gradual formation of a black precipitate was observed. The suspension was centrifuged at 2500 rpm for 5 minutes to separate the solid phase. In this one-pot green synthesis, polyphenolic compounds from guava extract first chelate with Fe^{2+} and Ni^{2+} ions. These polyphenols donate electrons to reduce the metal ions to lower oxidation states, inducing nucleation of Fe-Ni nanoparticles (Villagrán, Z. et al. 2024). Concurrently, oxidized polyphenols adsorb to the nanoparticle surfaces, acting as capping agents that prevent aggregation and provide a stable organic shell (Singh, J. et al. 2018). The resulting precipitate was collected by filtration through a 0.45 µm glass fiber filter, then oven-dried at 60°C for 48 hours to obtain the Fe-Ni bimetallic material (Villagrán, Z. et al. 2024). After drying, the material was cooled in a desiccator, ground into fine powder using a mortar and pestle, and stored under vacuum for subsequent experiments.

Adsorption experiments for Cu removal: In this study, a Cu solution with an initial concentration of 5 mg/L was selected, corresponding to 50 times higher than the permissible limit set by QCVN 08:2023/BTNMT (0.1 mg/L for Cu, the maximum allowable concentration for human health protection). Adsorbent dosages of 0.04 g/L, 0.08 g/L, and 0.12 g/L were investigated. The experiments were carried out using 0.01, 0.02, 0.03 g of Fe-Ni material for 25 mL sample solution (equivalent to material doses of 0.4, 0.8, and 1.2 g/L, respectively, respectively). Since $Cu(OH)_2$ begins to precipitate at pH 7, adsorption experiments were conducted at pH values of 1, 2, 3, 4, 5, 6, and 7, which were adjusted using 0.1 M HNO_3 and 0.1 M NaOH solutions. The optimal conditions were determined and applied in subsequent experiments. The effect of contact time was examined at intervals of 15, 30, 60, 90, 120, 150, 180, and 210 minutes. The effect of temperature was evaluated at 25°C, 30°C, 35°C, 40°C, 45°C, 50°C, and 55°C.

Characterization and analytical methods: The morphological characteristics of the adsorbent before and after Cu adsorption were analyzed using SEM, EDS, XRD, and FTIR. Cu concentrations were determined by molecular absorption spectrophotometry according to Hach Method 8506.

Data processing: Experimental data were processed using Microsoft Excel to calculate mean values and standard deviations. Statistical differences were analyzed using independent t-tests, and graphs were plotted with Origin software.

3. Results and discussion

3.1. Material morphology

Morphology and SEM images of the material: The synthesized material was obtained in the form of a fine powder with a dark greenish black color.

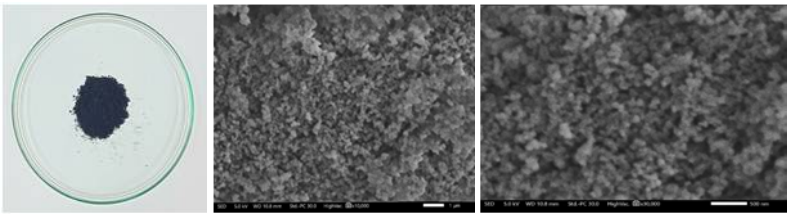

Figure 1. Photograph of the material (left), SEM image at a resolution of 1 µm (center), and SEM image at a resolution of 500 nm (right)

The SEM images reveal that the material exhibits limited dispersion and tends to aggregate into larger particles. The aggregation is attributed to the magnetic interactions between Fe and Ni particles. The particle sizes are heterogeneous, with an average diameter in the range of 60-90 nm within the nanoscale.

EDS spectrum: The EDS analysis revealed that the material was composed of C (52.5%), O (33.6%), Fe (10.2%), Ni (2.0%), P (0.7%), S (0.7%), and Cl (0.4%). These results confirm the presence of Fe and Ni in the material. The detection of Cl and S originates from the use of $NiCl_2$ and $FeSO_4$ during the synthesis, while the presence of P can be attributed to the guava leaf extract. These findings are consistent with the results reported by Yuanqiong Lin et al. (2019), in which Fe-Ni materials synthesized from 30 g of eucalyptus leaves contained Fe (11.83 wt%) and Ni (0.67 wt%).

Based on the standard reduction potentials of Fe^{2+}/Fe^0 (-0.44 V) and Ni^{2+}/Ni^0 (-0.25 V), Fe^{2+} is more easily reduced under the same conditions. During the reaction, Fe^{2+} is reduced and precipitates faster, thereby dominating the composition of the material. In addition, polyphenols, which contain multiple phenolic (-OH) and carbonyl groups, tend to form more stable complexes with Fe^{3+}/Fe^{2+} than with Ni^{2+}.

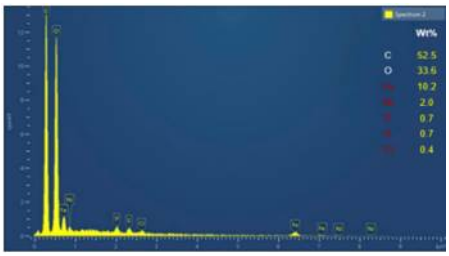

Figure 2. EDS spectrum of the material

Upon exposure to air, Fe^{2+} is readily oxidized to Fe^{3+}, which has a high affinity for polyphenols (forming dark brown complexes similar to tannin tests). These complexes may rapidly condense, yielding Fe-rich particles, which hinders the incorporation of Ni^{2+}. The relatively high proportions of C and O indicate that polyphenols from guava leaf extract are present on the material's surface.

FT-IR spectrum: The FT-IR spectrum exhibited several characteristic absorption peaks. The band at 3335.35 cm^{-1} corresponds to -OH groups of polyphenols, while the band at 1612.89 cm^{-1} is attributed to the C=C stretching vibrations of the aromatic ring. The C-H stretching vibration was observed at 1338.45 cm^{-1}. Other notable peaks include C-N at 1051.98 cm^{-1}, indicating the presence of amine groups derived from the plant extract, and C=O at 1178.34 cm^{-1}, characteristic of carbonyl groups in polyphenols. Inorganic bonds were also identified, including C-Cl (762.39 cm^{-1}), Fe-O (604.1 cm^{-1}), and Ni-O (513.73 cm^{-1}). The simultaneous presence of Fe-O and Ni-O absorption bands confirms the incorporation of both Fe and Ni into the material.

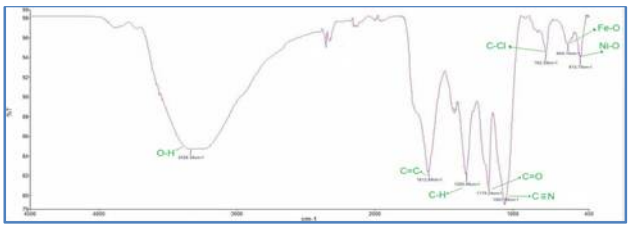

Figure 3. FT-IR spectrum of the material

3.2. Copper removal performance and adsorption mechanism

The EDS spectrum of the material after Cu adsorption showed a marked change in elemental composition. The appearance of Cu on the material surface resulted in a decrease in the mass percentages of several elements, with Fe and Ni decreasing by 1.0% and 0.8%, respectively. Similarly, C, S, and P contents also decreased. In contrast, the oxygen content increased, which can be attributed to the partial oxidation of the material into FeOOH, Fe_2O_3, $Ni(OH)_2$, and other oxides/hydroxides covering the surface (Yuanqiong Lin et al., 2019). The adsorption mechanism of Cu can be explained by both adsorption and reduction processes. The Fe-Ni surface, including its oxidized forms (oxides and hydroxides), provides a large surface area and numerous active sites where Cu^{2+} ions are adsorbed through electrostatic interactions with negatively charged functional groups such as -OH and $-O^-$. Metal organic complexes can also form through coordination bonding between metal ions and organic ligands (Zhou, B. et al., 2024, Villagrán, Z. et al. 2024). Accordingly, on the material surface, coordination bonds of Cu^{2+} with hydroxyl groups or oxo-metal groups are formed. This represents

the dominant mechanism under conditions where partial oxidation has occurred, resulting in the presence of FeOOH, Fe_2O_3, $Ni(OH)_2$, and -OH groups from guava leaf polyphenols on the surface.

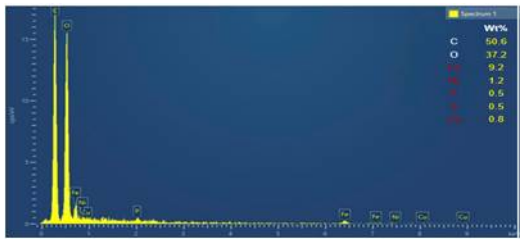

Figure 4. EDS spectrum of the material after Cu adsorption

Moreover, the surface of the Fe-Ni material is coated with biomacromolecules in molecular form (Yan et al., 2019, Villagrán, Z. et al. 2024), which partly protect the material from oxidation. As a result, a portion of Fe or Ni remains in metallic form (Fe^0, Ni^0), which can reduce Cu^{2+} to Cu^0: $Fe + Cu^{2+} \rightarrow Fe^{2+} + Cu\downarrow$; $Ni + Cu^{2+} \rightarrow Ni^{2+} + Cu\downarrow$. This mechanism leads to the precipitation of metallic Cu on the material surface. However, the efficiency of this process decreases over time due to the formation of oxide/hydroxide layers covering the metallic surface. Consequently, only a portion of Cu is reduced and converted to its zero-valent state (Zhou, B. et al., 2024).

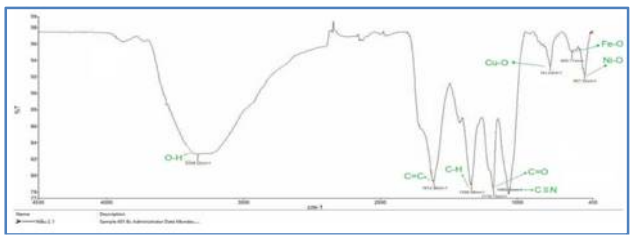

Figure 5. FT-IR spectrum of the material after Cu adsorption

The FT-IR spectrum after adsorption exhibited significant changes compared with that before adsorption. Notably, in the characteristic vibration region of metal-oxygen bonds, a new absorption peak corresponding to Cu-O was observed. This result confirms that Cu^{2+} ions were bound to the material through interactions with oxygen rich functional groups (-OH) derived from polyphenols.

3.3. Effect of initial pH

Since $Cu(OH)_2$ begins to precipitate at pH 7, the study was conducted only at pH values of 1, 2, 3, 4, 5, 6, and 7. The experiments were carried out using adsorbent doses of 0.4, 0.8, and 1.2 g/L, with a contact time of 150 minutes at 25°C. The results indicated that at low pH values (1-3), the removal efficiency was below 20% due to the dissolution of the material under acidic conditions (Wong et al., 2015). Regarding material dosage, an increase from 0.4 to 0.8 g/L significantly enhanced Cu(II) removal efficiency, mainly due to the greater number of available active sites and larger specific surface area for adsorption with more binding sites per volume (Popoola et al. 2024). Nevertheless, a further increase to 1.2 g/L did not yield a corresponding improvement. The results showed that the material dosage of 0.8 g/L at pH 6 achieved the highest efficiency (77.6%) compared with the other two dosages (41.4%, 70.4%). This phenomenon has been observed in many adsorption systems, and is often attributed to particle aggregation or overlapping of active sites at high adsorbent loading, which effectively reduces the accessible surface (Al-Ahmari et al. 2025); Chen et al. (2024) also mention that with higher dosages, collisions among particles and agglomeration become more probable, leading to a reduction in overall accessible surface and adsorption efficiency. The optimal performance at 0.8 g/L can thus be understood as the balance between providing sufficient adsorption sites and maintaining good dispersion of Fe/Ni particles, before the onset of excessive aggregation or site overlap. Therefore, 0.8 g/L was identified as the optimal adsorbent dosage for Cu(II) removal under the tested conditions. The efficiency increased markedly as the pH rose from 4 to 6, reaching an optimum of 77.6% at pH 6. At pH 7, the efficiency decreased because Cu began to precipitate as $Cu(OH)_2$, and hydroxide layers simultaneously started to form on the surface of the material under alkaline conditions.

pH is a critical factor in controlling Cu removal by Fe-Ni materials in aqueous solutions, as it influences both the contaminant and the surface charge of the adsorbent. These findings are consistent with those of Yuanqiong Lin et al. (2019), who reported that Cu removal efficiency increased from 9.4% to 44.9% as pH rose from 2 to 6, demonstrating that low pH impedes Cu removal. Therefore, an optimal pH of 6 and an adsorbent dosage of 0.8 g/L were selected for subsequent experiments.

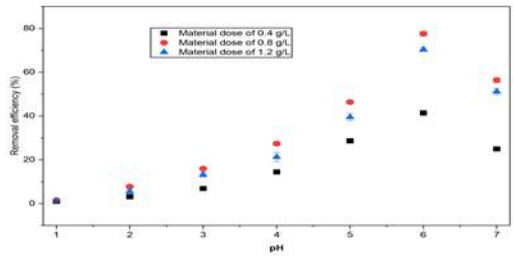

Figure 6. Effect of pH and optimal dosage

3.4. Effect of contact time

Batch experiments were conducted using 25 mL of Cu solution (5 mg/L) with an adsorbent dosage of 0.08 g/L at pH 6, contact times ranging from 15 to 180 minutes, and a temperature of 25°C.

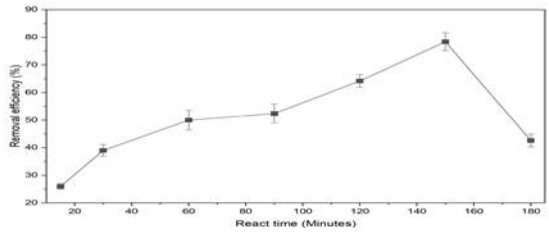

Figure 7. Effect of contact time

The results showed that removal efficiency varied with time. Within the first 90 minutes, the efficiency fluctuated, reaching only 50-52.4% indicating a slow adsorption process. However, between 90 and 150 minutes, the efficiency increased sharply, reaching an optimum of 78.4% at 150 minutes. After this point, the efficiency decreased to about 54% of the maximum at 180 minutes. In the initial stage, the active sites on the Fe-Ni surface coated with polyphenols remained available, allowing Cu^{2+} ions to readily access and bind through coordination with -OH and -COOH groups of polyphenols. In addition, reduction interactions occurred, where Ni^0 or Fe^0 partially reduced Cu^{2+} to Cu^0 deposited on the surface (Yuanqiong Lin et al., 2019).

The efficiency increased rapidly until approaching equilibrium. After reaching the maximum, the efficiency declined, possibly due to surface saturation and coverage, where adsorption sites became occupied by Cu^{2+} or reduced Cu^0. This coverage blocked underlying active sites, reducing further adsorption. Meanwhile, oxidation transformed the Fe-Ni surface during contact with the solution, producing Fe^{2+}/Fe^{3+} and Ni^{2+}. Hydroxide layers such as $Fe(OH)_3$ and $Ni(OH)_2$ may form surface coatings that inhibit new adsorption and reduction processes. Beyond the maximum adsorption point, desorption occurred: polyphenols were partially oxidized, reducing their ability to bind Cu^{2+}, which may have caused some previously adsorbed Cu to dissolve back into the solution (Yuanqiong Lin et al., 2019).

3.5. Effect of temperature

Experiments were performed with 5 mg/L Cu solution at pH 6, using 0.8 g/L of Fe-Ni material, with an adsorption time of 150 minutes, at six different temperatures ranging from 25 to 55°C. The results revealed that adsorption efficiency decreased with increasing temperature, with the optimum removal efficiency of 79% achieved at 25°C, and then declined significantly with further increases in temperature. These findings indicated that Cu adsorption is an exothermic process. At higher temperatures, less Cu is retained in the solid phase resulting in reduced adsorption capacity (Yue, Y. et al., 2025). Furthermore, elevated temperatures increase the kinetic energy of ions in solution, while the weakening of coordination interactions at high temperatures also reduces adsorption efficiency (Zhang, W.L. et al., 2019). In addition, polyphenols may lose stability at elevated temperatures (Teng, X. et al., 2024) leading to structural changes or detachment from the surface, leading to the loss of functional groups such as -OH and -C=O that are essential for Cu binding (A.A.K.K. Rikabi et al., 2024).

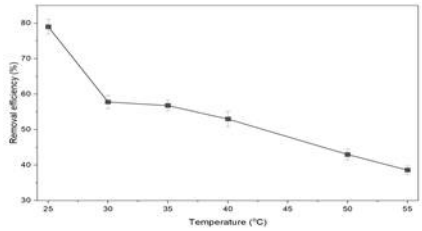

Figure 8. Effect of temperature on removal efficiency

4. Conclusion

In this study, Fe-Ni nanomaterials with particle sizes ranging from 60 to 90 nm were successfully synthesized using guava leaf extract. The material was coated with polyphenols from guava leaf extract and demonstrated effective Cu removal through combined adsorption and reduction mechanisms. These findings were supported by EDS and FT-IR analyses. The optimal conditions for Cu removal at an initial concentration of 5 mg/L were determined to be pH 6, an Fe-Ni dosage of 0.8 g/L, a temperature of 25°C, and an adsorption time of 150 minutes, achieving a maximum removal efficiency of 79%. These findings highlight the practical significance of this research in minimizing the use of hazardous chemicals and promoting green synthesis of environmentally friendly materials for wastewater treatment.

References

Abbas, A. K. K. R., Alzubadiy, M. W. M., Ali, Z. H., Khudhair, H. M., & Abdulhasan, M. J., 2024. *Optimization of ecofriendly L-Fe-Ni nanoparticles prepared using extract of black tea leaves for removal of tetracycline antibiotics from groundwater by response surface methodology.* South African Journal of Chemical Engineering, 50, 89-99. https://doi.org/10.1016/j.sajce.2024.07.007

Al-Ahmari JM, Alghanmi RM, Hamouda RA., 2025, *Bio-Fabricated Aluminum Oxide Nanoparticles Derived from Waste Pharmaceutical Packages: Insight into Characterization and Applications.* Biomolecules. Jul 10;15(7):984. doi: 10.3390/biom15070984

Gao, J. F., Wu, Z. L., Duan, W. J., & Zhang, W. Z., 2019. *Simultaneous adsorption and degradation of triclosan by Ginkgo biloba L. stabilized Fe-Co bimetallic nanoparticles.* Science of the Total Environment, 662, 978-989. https://doi.org/10.1016/j.scitotenv.2019.01.194

Hanjie Chen, Mei Zhang, Shuyang Chen and Ying Fang, 2024, *Study adsorbents based on bent-Al13-CS-CTA and its application to the removal of CR from wastewater*, RSC Adv., 14,13817, DOI: 10.1039/D4RA00197D

Hamdi, M. F., 2025. *Advanced remediation of toxic materials using zero-valent iron nanoparticles: A comprehensive review.* Water, Air, & Soil Pollution, 236, 780. https://doi.org/10.1007/s11270-025-08420-1

Khodadad Kavosi Rakati, Masoomeh Mirzaei, Sarah Maghsoodi, Amirhossein Shahbazi, 2019. *Preparation and characterization of polyaniline-modified chitosan embedded with ZnO-Fe3O4 for Cu(II) removal from aqueous solution*, International Journal of Biological Macromolecules, Volume 130, Pages 1025-1045, ISSN 0141-8130, https://doi.org/10.1016/j.ijbiomac.2019.02.033.

Sewoon Kim, Kyoung Hoon Chu, Yasir A.J. Al-Hamadani, Chang Min Park, Min Jang, Do-Hyung Kim, Miao Yu, Jiyong Heo, Yeomin Yoon, 2018, *Removal of contaminants of emerging concern by membranes in water and wastewater: A review*, Chemical Engineering Journal, Volume 335, Pages 896-914, ISSN 1385-8947, https://doi.org/10.1016/j.cej.2017.11.044.

Le ND, Hoang TTH, Phung VP, Nguyen TL, Rochelle-Newall E, Duong TT, Pham TMH, Phung TXB, Nguyen TD, Le PT, Pham LA, Nguyen TAH, Le TPQ, 2022. *Evaluation of heavy metal contamination in the coastal aquaculture zone of the Red River Delta (Vietnam)*. Chemosphere. 2022 Sep; 303(Pt 1):134952. doi: 10.1016/j.chemosphere.2022.134952.

Yuanqiong Lin, Jin, X., Owens, G., & Chen, Z., 2019. *Simultaneous removal of mixed contaminants triclosan and copper by green synthesized bimetallic iron/nickel nanoparticles.* Science of the Total Environment, 695, 133878. https://doi.org/10.1016/j.scitotenv.2019.133878

Ministry of Natural Resources and Environment (MONRE) (2020), *National report on the state of the environment*, 2016-2020 period.

Phuong, D. T. L., 2024. *Green synthesis of iron nanoparticles from plants.* Journal of Water Resources & Environmental Engineering, 92(12/2024).

Popoola LT., 2024, Parameter Influence, *Characterization and Adsorption Mechanism Studies of Alkaline-Hydrolyzed Garcinia kola Hull Particles for Cr(VI) Sequestration.* Environ Health Insights. Jan 20;18:11786302231215667. doi: 10.1177/11786302231215667.

Singh, J., Dutta, T., Kim, KH. et al., 2018, *'Green' synthesis of metals and their oxide nanoparticles: applications for environmental remediation.* J Nanobiotechnol **16**, 84. https://doi.org/10.1186/s12951-018-0408-4

Teng, X., Xie, K., Yan, C., Wang, Z., & Qu, R., 2024. *Effect of small molecule phenolic compounds on the removal of triclosan (TCS) by heat/persulfate process: Formation of cross coupling products and implications for wastewater treatment.* Chemical Engineering Journal, 488, 150966. https://doi.org/10.1016/j.cej.2024.150966

USEPA., 2021. *National Recommended Water Quality Criteria - Aquatic Life Criteria Table.* United States Environmental Protection Agency.

Van Thinh, N., Chung, N.T., Luong, L.T.M. et al., 2022, *Assessment of total concentrations of heavy metals in industrial sludges from the North of Vietnam and their potential impact on the ecosystem.* Environ Sci Pollut Res 29, 42055-42066; https://doi.org/10.1007/s11356-021-17619-8

Villagrán, Z., Anaya-Esparza, L. M., Velázquez-Carriles, C. A., Silva-Jara, J. M., Ruvalcaba-Gómez, J. M., Aurora-Vigo, E. F., Rodríguez-Lafitte, E., Rodríguez-Barajas, N., Balderas-León, I., & Martínez-Esquivias, F. (2024). *Plant-Based Extracts as Reducing, Capping, and Stabilizing Agents for the Green Synthesis of Inorganic Nanoparticles.* Resources, 13(6), 70. https://doi.org/10.3390/resources13060070

Weng, X. L., Guo, M. Y., Luo, F., & Chen, Z. L., 2017. *One-step green synthesis of bimetallic Fe-Ni nanoparticles by eucalyptus leaf extract: Biomolecules identification, characterization and catalytic activity*. Chemical Engineering Journal, 308, 904-911. https://doi.org/10.1016/j.cej.2016.09.134

Qinghua Xu, Yulu Wang, Liqiang Jin, Yu Wang, Menghua Qin, 2017. *Adsorption of Cu (II), Pb (II) and Cr (VI) from aqueous solutions using black wattle tannin-immobilized nanocellulose,* Journal of Hazardous Materials, Volume 339, 2017, Pages 91-99, ISSN 0304-3894, https://doi.org/10.1016/j.jhazmat.2017.06.005.

Yan, Z. R., Meng, H. S., Yang, X. Y., Zhu, Y. Y., Li, X. Y., Xu, J., & Sheng, G. P., 2019. *Insights into the interactions between triclosan (TCS) and extracellular polymeric substance (EPS) of activated sludge.* Journal of Environmental Management, 232, 219-225.

Youssif, M. M., El-Attar, H. G., Hessel, V., & Wojnicki, M., 2024. *Recent developments in the adsorption of heavy metal ions from aqueous solutions using various nanomaterials.* Materials, 17(21), 5141. https://doi.org/10.3390/ma17215141

Yue, Y., Adhab, A. H., Sur, D., 2025. *Thermodynamic modeling adsorption behavior of a well-known gelation crosslinker on sandstone rocks.* Scientific Reports, 15, 22544. https://doi.org/10.1038/s41598-025-06005-w

Zhang, W. L., Oswal, H., Renew, J., Ellison, K., & Huang, C. H., 2019. *Removal of heavy metals by aged zero-valent iron from flue-gas-desulfurization brine under high salt and temperature conditions.* Journal of Hazardous Materials, 373, 572-579.

Zhou, B., Fan, B., Gong, Z., Shao, S., Zhou, D., & Gao, S., 2024. *Optimized preparation of Ni-Fe bimetallic particles by ball milling $NiSO_4$ and iron powder for efficient removal of triclosan.* Chemosphere, 360, 142359. https://doi.org/10.1016/j.chemosphere.2024.142359